reliable assessment of this association constant, we observed a downfield shift in contrast to Mg^{2+} and Ca^{2+}. The crystallographic literature predicts this also. Bond angles increase in Ba^{2+} salts.[32] Apparently, the greater cationic radius of Ba^{2+} (1.35 Å) as compared to the radii of Ca^{2+} and Mg^{2+} (0.99 and 0.65 Å) expands the O-P-O bond angle.

The association constants presented in Table IV are relatively small. They represent a difference of several kilocalories per mole between the unassociated and associated species. This results from association, not between naked ions but between strongly solvated species.[33,34] Therefore, association involves the replacement of several water molecules by one ion. The difference in the free energy changes between equilibria with equilibrium constants of 0.1 and 30, for example, is less than 3.5 kcal/mol. This indicates that the total solvation of the divalent ions is comparable in energy to the Coulombic attraction of divalent counterions. In this regard, it is interesting that our values in Table IV for dication-phosphate monoanion association are very similar to the values in Tables II and III for monocation-phosphate dianion association.

The previously unmeasured stability constants for association of monocations with the dimethyl phosphate monoanion and the cAMP monoanion appear to be within experimental error of 0.2 and 0.1 M^{-1}, respectively. These values are about an order of magnitude less than both monocation-dianion and dication-monoanion association constants which, in turn, are about an order of magnitude less than the dication-dianion association constants. The nucleoside phosphate, cAMP monoanion, has consistently lower metal cation association constants than the dimethyl phosphate monoanion and different $\Delta\delta_{max}$ values. In contrast, the stability constants and $\Delta\delta_{max}$ values of ethyl phosphate and AMP are nearly all within experimental error of each other. This is most likely due to some effect of the six-membered phosphate-containing ring. Possible causes include an abnormal O-P-O angle or the water molecule that is known to be bound to the 2'-hydroxyl and phosphoryl oxygens.[4]

The results of guanidinium ion association demonstrate little difference between guanidinium ion and metal cations. There is consistency of the $\Delta\delta_{max}$ and K values for dimethyl phosphate and cAMP association. We previously measured the constant for association of the guanidinium ion to bis(nitrophenyl) phosphate and determined K to be 0.18 M^{-1} by a kinetic method.[35] This is in excellent agreement with our NMR results in Table II. Dianion association to the guanidinium ion shows an appreciable increase in affinity over that to the metal monocations. This is presumably due to the ability of guanidinium ions to hydrogen bond and thereby enhance the electrostatic interaction.

The results in Table IV indicate our NMR method is revealing inner-sphere complexation. This conclusion is drawn from the specific effects individual cations bring about. The most notable of these effects is the change in direction of the chemical shift incurred upon binding monocations vs. dications. The $\Delta\delta_{max}$ values for dications are similar but very different from those for monocations. The relative K values also fit for changes in charges of the complexing ions as mentioned above. In fact, it seems likely that a major advantage of this method is the much larger effects of inner-sphere complexation over outer-sphere effects that may interfere in other methods for the determination of association constants.

Future applications of this method will include an examination of the sites of coordination of cations to nucleoside polyphosphates and a measurement of constants for association to polynucleotides.

Registry No. DMP^-, 7351-83-9; $cAMP^-$, 62906-31-4; AMP^{2-}, 6042-43-9; Mg, 7439-95-4; Ca, 7440-70-2; Li, 7439-93-2; Na, 7440-23-5; K, 7440-09-7; $C(NH_2)_3^+$, 25215-10-5; ethyl phosphate, 57919-10-5.

(32) Kyogoku, Y.; Iitaka, Y. *Acta Crystallogr.* **1966**, *21*, 49-57.
(33) Gurney, R. W. "Ionic Processes in Solution"; McGraw-Hill: New York, 1953; pp 264-265.
(34) Nancollas, G. H. "Interactions in Electrolyte Solutions"; Elsevier: New York, 1966; p 10.
(35) Springs, B.; Haake, P. *Tetrahedron Lett.* **1977**, 3223-3226.

Contribution from the Laboratoire de Chimie-Physique CSP, Université Paris-Nord, 93430 Villetaneuse, France

Low-Frequency IR and Raman Spectra of $Mn(CO)_3(\eta^5\text{-}C_5H_5)$ and $Re(CO)_3(\eta^5\text{-}C_5H_5)$. Study of Dynamic Disorder

K. CHHOR*† and G. LUCAZEAU

Received December 1, 1982

Low-frequency Raman (5-200 cm^{-1}) and infrared spectra (20-200 cm^{-1}) of $Mn(CO)_3(\eta^5\text{-}C_5H_5)$, $Re(CO)_3(\eta^5\text{-}C_5H_5)$, and the deuterated ($d_5$) derivative of the Mn complex have been reported in the 5-300 K temperature range. A complete assignment for the low-frequency modes is proposed; their temperature dependence is discussed in terms of anharmonicity and vibrational dephasing associated with large amplitude motions. A potential barrier of 10 kJ mol^{-1} at 300 K is deduced from the torsional frequency; it is compared with the activation energy found by quasi-elastic neutron scattering and by NMR.

I. Introduction

This work has been undertaken as a part of a general study of the mechanism involved in the order-disorder phase transitions occurring in metallocenes and arene metal carbonyls.[1-8] From Raman and neutron scattering we have shown that aromatic rings are able to undergo jumps in the solid state and that the associated potential barrier is between 4 and 16 kJ mol^{-1} for most of these compounds; these values agree generally well with NMR results. We have recently used incoherent quasi-elastic neutron scattering (IQNS) to study the

†ERA CNRS No. 456.

(1) Chhor, K. Thèse Doctorat d'Etat, Université Paris XIII, 1982.
(2) Chhor, K.; Sourisseau, C.; Lucazeau, G. *J. Raman Spectrosc.* **1981**, *11*, 183.
(3) Chhor, K.; Lucazeau, G. *J. Raman Spectrosc.* **1982**, *13*, 235.
(4) Chhor, K.; Lucazeau, G. *Spectrochim. Acta, Part A* **1982**, *38A*, 1163.
(5) Chhor, K.; Sourisseau, C.; Lucazeau, G. *J. Mol. Struct.* **1982**, *80*, 485.
(6) Sourisseau, C.; Lucazeau, G.; Dianoux, A. J.; Poinsignon, C. *Mol. Phys.* **1983**, *11*, 1.
(7) Lucazeau, G.; Chhor, K.; Sourisseau, C.; Dianoux, A. *Chem. Phys.* **1983**, *76*, 307.

0020-1669/84/1323-0462$01.50/0

C_5H_5 motions in $Mn(CO)_3(\eta^5\text{-}C_5H_5)$;[7] in this case, the activation energy (16.8 kJ mol^{-1}) and the correlation time (1.7×10^{-11} s) are somewhat different from the values (7.2 kJ mol^{-1} and 6.4×10^{-13} s) deduced from the spin-lattice relaxation time T_1.[9]

We present here the Raman and IR results on $Mn(CO)_3(\eta^5\text{-}C_5H_5)$ (CpMnT) and its isomorph $Re(CO)_3(\eta^5\text{-}C_5H_5)$ (CpReT). A part of these results have already been presented.[10] The two compounds have been extensively studied in the past. Their structure has been redetermined recently,[11] and the distortion of the C_5H_5 ring has been underlined. The same conclusion was obtained from spectroscopic studies.[12-15] However the low-frequency region of these complexes has not yet been interpreted; in particular, neither the torsional mode nor the librational mode has been identified. Therefore we have undertaken the vibrational study of the low-frequency region in order to characterize these modes and to estimate the corresponding potential barriers. Moreover the distortion of C_5H_5 ring as determined by X-ray studies creates a favorable situation for the observation of these modes, the activity of which is likely enhanced. Finally the aim of this work was to study the temperature dependence in the 10–300 K temperature range and to contribute to the knowledge of the dynamic disorder. The existence of a phase transition taking place between 77 and 300 K has been controversial.[12,16] The variations of lattice parameters as a function of temperature do not present discontinuities that could indicate the existence of such a phase transition.[17] However C_p measurements[1,18] reveal a small anomaly at about 100 K which was not interpreted in terms of disorder as for $(\eta^5\text{-}C_5H_5)_2Ni$. No conclusion was reached as to the existence of distinguishable configurations in the crystal. However this anomaly could indicate that a weak second-order phase transition takes place. This point can be examined by studying the external modes that are expected to be the most sensitive to a slight structural change.

II. Experimental Section

Samples. $Mn(CO)_3(\eta^5\text{-}C_5H_5)$ and $Re(CO)_3(\eta^5\text{-}C_5H_5)$ were commercially obtained; the samples were purified by repeated sublimations in vacuum before use. The $Mn(CO)_3(\eta^5\text{-}C_5D_5)$ derivative was prepared by repeated isotopic exchange reactions between $Mn(CO)_3(\eta^5\text{-}C_5H_5)$ and $Sr(OD)_2$ at 230 °C according to the method described by Parker et al.[13] The isotopic purity estimated by NMR is greater than 85%.

Raman and IR Spectrometers. Raman experiments were performed with a Coderg T800 triple monochromator spectrometer equipped with an ionized argon laser (4880 and 5145 Å). The low-temperature measurements were obtained by using a liquid helium cryostat. Thermocouple readings as well as Stokes–anti-Stokes ratios were used to estimate the sample temperature.

Infrared spectra were recorded on a FIR 30 Polytec interferometer in the 20–300 cm^{-1} frequency range. Polycrystalline samples were dispersed in Nujol.

III. Structure and Selection Rules

1. Isolated Molecule. The most probable conformation for $Mn(CO)_3(\eta^5\text{-}C_5H_5)$ (CpMnT) is likely staggered (Figure 4) and belongs to the point group C_s. The $Mn(\eta^5\text{-}C_5H_5)$ and $Mn(CO)_3$ moieties have C_{5v} and C_{3v} local symmetry, respectively. Assuming a weak interaction between C_5H_5 and $Mn(CO)_3$ groups, Lippincott et al.[16] have interpreted the vibrational spectra of CpMnT on the basis of such local symmetry. However these assumptions have been criticized by several authors. From vibrational[12-14] and NMR[15] studies of CpMnT in solution, it has been concluded that the C_5H_5 ring undergoes a significant distortion and that its symmetry is only C_{2v}. The same conclusion was also reported for $Re(CO)_3(\eta^5\text{-}C_5H_5)$ (CpReT) from a vibrational study.[19] Under these conditions, the spectra of these compounds must be interpreted on the basis of the molecular point group C_s.

Table I. IR and Raman Selection Rules and Activities of Low-Frequency Modes

vib modes at freq <200 cm^{-1}	molecular group C_s	site symmetry C_1	factor group C_{2h} ($Z = 4$)
T'_z	A′	A	$1A_g + 1B_g + 1A_u{}^a + 1B_u$
$T'_{x,y}$	A′ + A″	2A	$2A_g + 2B_g + 2A_u + 2B_u{}^a$
R'_z	A″	A	$1A_g + 1B_g + 1A_u + 1B_u$
$R'_{x,y}$	A′ + A″	2A	$2A_g + 2B_g + 2A_u + 2B_u$
τ_z	A″	A	$1A_g + 1B_g + 1A_u + 1B_u$
δ(CMC)	2A′ + A″	3A	$3A_g + 3B_g + 3A_u + 3B_u$
δ(R-M-$(CO)_3$)	A′ + A″	2A	$2A_g + 2B_g + 2A_u + 2B_u$

[a] Three acoustic modes must be subtracted.

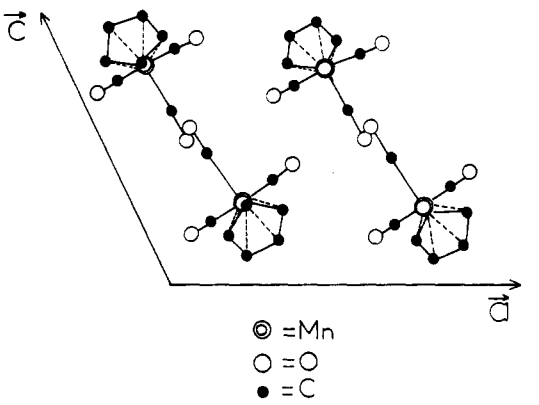

Figure 1. (010) projection of the crystal structure of $Mn(CO)_3(\eta^5\text{-}C_5H_5)$.

The three $M(CO)_3$ group bending modes and the three modes corresponding to ring–$M(CO)_3$ relative motions are known to occur below 200 cm^{-1} [12-14] and can be classified as $3A' + 3A''$ representations of the C_s group.

2. Molecule in the Crystal. Crystallographic studies at 300 K have shown that the CpMnT[11,20] and CpReT[21] molecules are located in sites of C_1 symmetry. The C_5H_5 rings are planar. However, as for the isolated state, the deviation from D_{5h} regular pentagonal symmetry is observed for both compounds. The C–C bond distances of the ring reported by Fitzpatrick et al.[11,21] range from 1.40 to 1.44 Å.

As shown in Table I, the number of Raman and IR bands expected for the molecule in the crystal is the same as for the isolated molecule of C_s symmetry.

3. Crystal Structure. All crystallographic studies performed at 300 and 77 K have concluded that CpMnT and CpReT crystals belong to the monoclinic system with four molecules per unit cell related to each other through the symmetry op-

(8) Chhor, K.; Pommier, C.; Berar, J. F.; Calvarin, G.; Diot, M. *Mol. Cryst. Liq. Cryst.* **1981**, *71*, 3.
(9) Fitzpatrick, P. J.; Gilson, D. F. R.; Gomez, G.; Butler, I. S., unpublished results.
(10) Chhor, K.; Pommier, C.; Lucazeau, G., presented in part at the IX International Conference Organometallic Chemistry Dijon, France, Sept., 1979.
(11) Fitzpatrick, P. J.; Le Page, Y.; Sedman, J.; Butler, I. S. *Inorg. Chem.* **1981**, *20*, 2852.
(12) Adams, D. M.; Squire, A. *J. Organomet. Chem.* **1973**, *63*, 381.
(13) Parker, D. J.; Stiddard, M. H. B. *J. Chem. Soc. A* **1970**, 480.
(14) Parker, D. J. *J. Chem. Soc. A* **1970**, 1382.
(15) Khetrapal, C. L.; Dunwar, A. C.; Saupe, A. *Mol. Cryst. Liq. Cryst.* **1976**, *35*, 215.
(16) Hyams, I. J.; Bailey, R. T.; Lippincott, E. R. *Spectrochim. Acta, Part A* **1967**, *23A*, 000.
(17) Berar, J. F. Thèse Doctorat d'Etat, Université Paris VI, 1980.
(18) Chhor, K.; Pommier, C.; Diot, M. *Mol. Cryst. Liq. Cryst.* **1983**, *100*, 193.
(19) Lokshin, B. V.; Menkova, Z. S. K.; Makarov, Yu. V. *Spectrochim. Acta, Part A* **1972**, *28A*, 2209.
(20) Berndt, A. F.; Marsh, R. E. *Acta Crystallogr.* **1963**, *16*, 118.
(21) Fitzpatrick, P. J.; Le Page, Y.; Butler, I. S. *Acta Crystallogr., Sect. B* **1981**, *B37*, 1052.

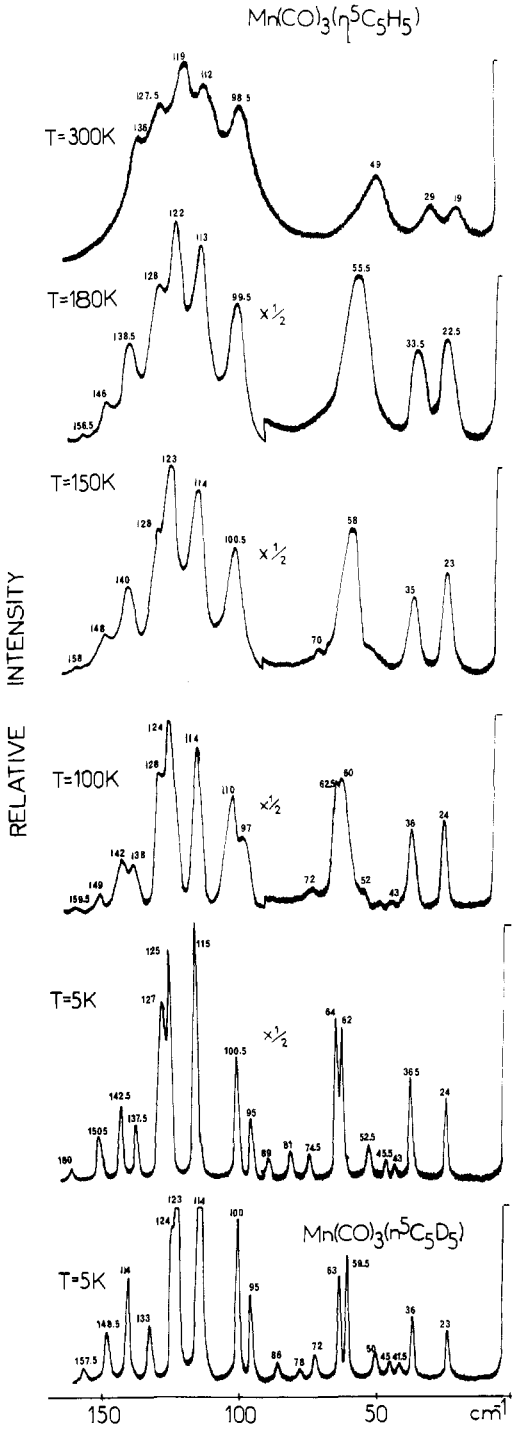

Figure 2. Low-frequency Raman spectra of $Mn(CO)_3(\eta^5\text{-}C_5H_5)$ between 5 and 300 K and the Raman spectrum of the d_5 derivative at 5 K (lowest spectrum).

erations of the space group $P2_1/a$ (Figure 1).[11,17,20,21] The correlation between molecular group C_s, C_1 site group, and C_{2h} factor group indicates that each vibrational molecular mode corresponds to two Raman and two IR bands. In the frequency range below 200 cm^{-1}, one expects 24 internal modes giving rise to 12 Raman and 12 IR active modes (Table I) and 21 external modes giving rise to 12 Raman and 9 IR active modes. On the assumption that librational and translational motions are not coupled and after substraction of acoustic modes, these external modes can be classified as follows:

$$\Gamma_R^{crystal} = 3A_g + 3B_g + 3A_u + 3B_u$$

$$\Gamma_T^{crystal} = 3A_g + 3B_g + 2A_u + 1B_u$$

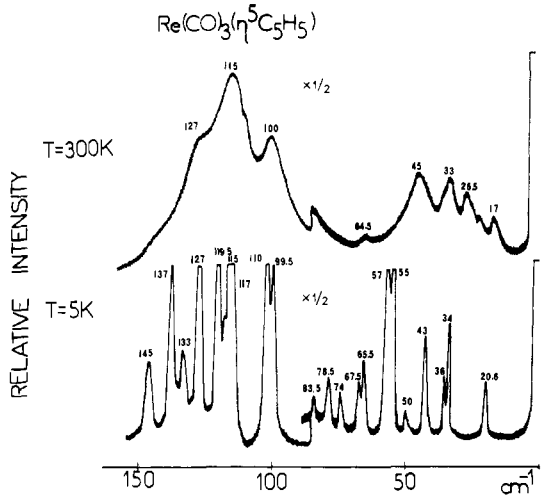

Figure 3. Low-frequency Raman spectra of $Re(CO)_3(\eta^5\text{-}C_5H_5)$ at 5 and 300 K.

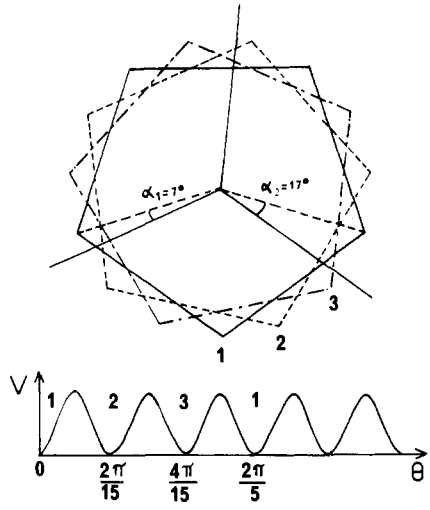

Figure 4. Molecular conformations of $Mn(CO)_3(\eta^5\text{-}C_5H_5)$: (1) full line, staggered conformation of C_s symmetry. (2, 3) dotted lines, $2\pi/15$ rotations of C_5H_5 ring. An intramolecular cosine potential function of period $n = 15$ is reported in the lower part of the figure.

IV. Results and Discussion

Figure 2 reports the Raman spectra of $Mn(CO)_3(\eta^5\text{-}C_5H_5)$ at different temperatures in the frequency range 5–200 cm^{-1}. The Raman spectrum of the corresponding d_5 derivative at 5 K is given in the same figure for comparison. $Re(CO)_3(\eta^5\text{-}C_5H_5)$ Raman spectra at 5 and 300 K are shown in Figure 3. The frequencies and assignments of the corresponding bands are reported in Table II. Figures 6 and 7 give the curves representing the variation of frequencies and half-widths of some bands for CpMnT in the temperature range 5–250 K.

1. Assignments of Spectra below 200 cm^{-1} and Structural Conclusions. As for other metal arene tricarbonyls, e.g., $Cr(CO)_3(\eta^6\text{-}C_6H_6)$[3] and $Cr(CO)_3(\eta^5\text{-}C_4H_4S)$,[4] the room temperature spectra of CpMnT and CpReT can be separated into two distinct regions: the first one, below 95 cm^{-1}, corresponds to the external and torsional modes, and the second one, between 95 and 160 cm^{-1}, represents the bending internal modes of the molecule.

a. The low-temperature Raman spectra (5 K) for both complexes, below 95 cm^{-1}, exhibit nine bands instead of the ten expected for the C_{2h} factor group with $Z = 4$ (Table I).

For CpMnT, the Raman bands at 160, 150.5, and 137.5 cm^{-1}, which shift noticeably on deuteration of the ring, are assigned as for $Cr(CO)_3(\eta^6\text{-}C_6H_6)$[3] to bending modes δ(R–M–$(CO)_3$). The 142.5-cm^{-1} band, although less sensitive, must

Table II. Low-Frequency Modes of CpMnT, CpMnT-d_5, CpReT

$Mn(CO)_3(\eta^5\text{-}C_5H_5)$							$Re(CO)_3(\eta^5\text{-}C_5H_5)$					
IR		Raman				$\rho(h_5/d_5)^a$	Raman		ρ(CpMnT/		symmetry	
300 K	100 K	300 K	100 K	5 K	5 K[b]	5 K	300 K	5 K	CpReT)[a]	assignment	C_s	C_{3v}
		19	24	24	23	1.04	17	20.5	1.17	T'		
		29	36	36.5	36	1.014	26.5	34	1.07	T'		
39	42		43	43	41.5	1.036		36	1.19	R'	A' or A''	
		47	45.5	45	1.011	33	43	1.06	T'			
			52.5	50	1.05	45	50	1.05	R'_z	A''		A_2
		60	62	63	0.98		55	1.13	T'	A' or A''		
		~55	62.5	64	59.5	1.076		57	1.12	τ_z	A''	A_2
		48						65.5		R'		
67	69		72	74.5	72	1.035	64.5	67.5	1.06			
74	75			81	78	1.038		74	1.09	R'	A' or A''	
								78.5				
			83	89	86	1.035		83.5	1.066	R'		
			97	95	95	1.00		99.5				
		98	101	100.5	100	1.00	100	101.5		δ(CMC)	A'	A_1
	111	112.5	114.5	115	114	1.01		115		δ(CMC)	A' or A''	E
122												
	124	119.5	124	125	123	1.016	115	117				
			128	127	124.5	1.02		119.5				
		127.5	138	137.5	133	1.034		127				
		136	142	142.5	141	1.01	127	133				
										δ(R-M(CO)$_3$)	A' or A''	E
			149	150.5	148.5	1.013		137				
145	145											
			159.5	160	157.5	1.016		145				

[a] See Table III for corresponding theoretical values. [b] Spectra of d_5 derivative.

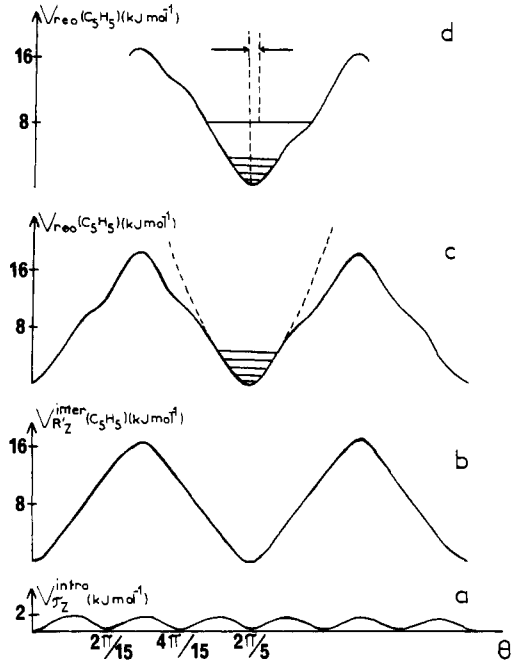

Figure 5. Qualitative representation of potential terms entering into eq 1 (see text): (a) intramolecular potential function $V_{\tau_z}^{intra}$ (V^o has been arbitrarily overestimated); (b) intermolecular potential function corresponding to the interactions between the rings and the surrounding atoms belonging to other molecules; (c) symmetric function resulting from the in phase addition of (a) and (b) (the averaged equilibrium position is the same for all vibrational levels); (d) asymmetric function resulting from the addition of (a) and (b) with a dephasing of 5° (the minima of (b) have been displaced 5°). The averaged equilibrium position is different for vibrational levels above and below $V^o_{reo} \simeq 8$ kJ mol^{-1}.

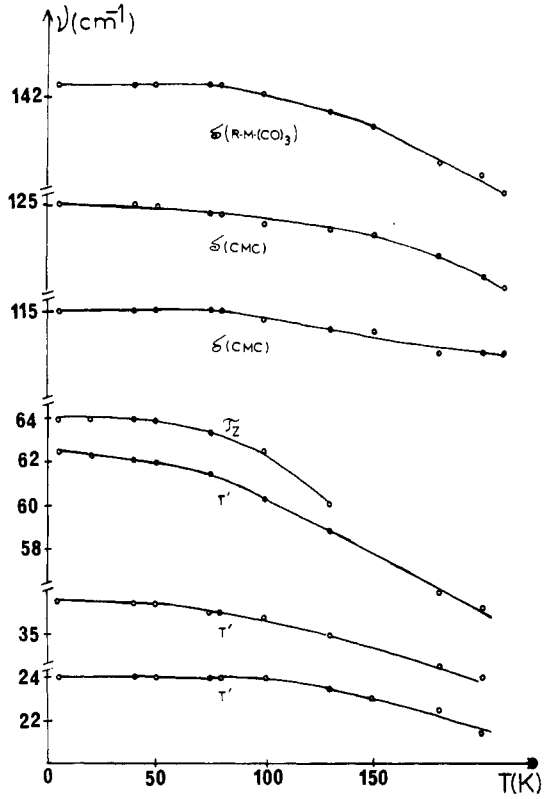

Figure 6. Temperature dependence of some low-frequency modes for $Mn(CO)_3(\eta^5\text{-}C_5H_5)$.

also belong to this mode, because if it was assigned to a δ(CMC) mode, this should imply a degeneracy removing of about 17 cm^{-1} and this should be much larger than that observed in $M(CO)_3(\eta^6\text{-}C_6H_6)$ complexes.[3] The isotopic insensitivity could be only apparent and masked by couplings with other modes. The Raman bands at 127, 125, 115, 100.5, and 95 cm^{-1} associated with the $M(CO)_3$ group (δ(CMC)) are less sensitive toward deuteration (Table II). In this region, Parker et al.[13] have reported in their Raman spectra at 77 K five

Table III. Moments of Inertia and Theoretical Isotopic Ratios[a]

compd	I_x	ρI_x	I_y	ρI_y	I_z	ρI_z	I_r	ρI_r	M	ρM
$Mn(CO)_3(\eta^5\text{-}C_5H_5)$	627.8		600.8		471.8		83.0		204	
		1.022		1.022		1.025		1.078		1.01
$Mn(CO)_3(\eta^5\text{-}C_5D_5)$	655.8		628		495.5		96.5		209	1.28
$Re(CO)_3(\eta^5\text{-}C_5H_5)$									335	
C_5H_5	51.9		55.6		107.5					
						1.1				
C_5D_5	63.5		67.8		131.2					

[a] I_x, I_y and I_z are the principal moments of inertia; I_r is the reduced moment for the torsional motion. All the moments are given in amu Å^2. For $Mn(CO)_3(\eta^5\text{-}C_5H_5)$ these values have been computed from the cartesian coordinates of atoms reported in ref 11 and 20. ρI_x, ρI_y, ρI_z: theoretical values associated with librations of the molecule around the x, y, and z axes, respectively. ρI_r: theoretical value associated with the torsional motion given by $[I_r(d_5)/I_r(h_5)]^{1/2}$. The theoretical value associated with the motion of rings alone is equal to $[I_z(C_5D_5)/I_z(C_5H_5)]^{1/2} = 1.1$. ρM: theoretical value associated with the translational motions of molecules given by $[M(d_5)/M(h_5)]^{1/2}$ and $[M(\text{CpMnT})/M(\text{CpReT})]^{1/2}$.

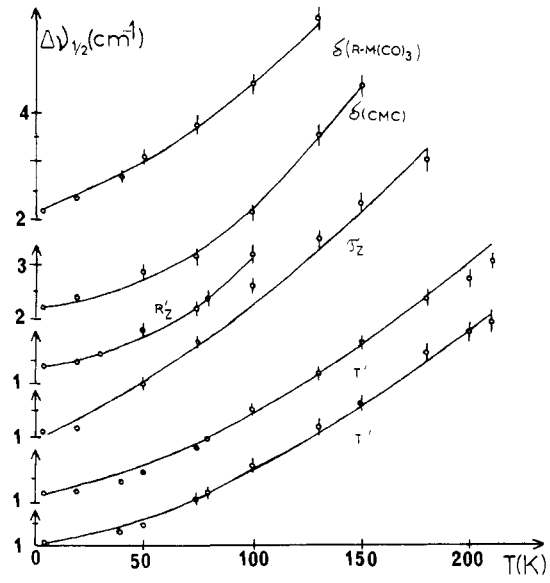

Figure 7. Temperature dependence of the half-width of some Raman active modes for $Mn(CO)_3(\eta^5\text{-}C_5H_5)$.

maxima, which they assigned to bending modes δ(CMC) and δ(R–M–$(CO)_3$), while Adams et al.[12] have reported seven maxima in this region without assignments.

For CpReT, by analogy with CpMnT, the Raman bands at 5 K at 119.5, 117, 115, 101.5, and 99.5 cm^{-1} are assigned to bending modes δ(CMC), while the remaining bands in this region at 145, 137, 133, and 127 cm^{-1} are associated with δ(R–M–$(CO)_3$) modes. Lokshin et al.[19] reported at 300 K three Raman bands in this region without assignments.

In the frequency range below 95 cm^{-1}, 14 Raman active modes (six librations, six translations, two torsions) and 11 IR active modes (six librations, three translations, two torsions) are expected (Table I). In fact, only 10 and 12 Raman bands are observed at 5 K for CpMnT and CpReT, respectively. On the basis of isotopic shifts, one can consider that the Raman bands with isotopic ratios ρ less than or equal to 1.02 should be associated with translational modes while those with ρ values equal or larger than 1.03 should correspond to librational R′ or torsional modes (Table III). The examination of CpMnT and CpMnT-d_5 derivative Raman spectra indicates that the bands at 24, 36.5, 45.5, and 64 cm^{-1} can be assigned to T′ modes and those at 43, 62, 74.5, 81, 89, and 52.5 cm^{-1} correspond to R′ and τ_z modes respectively. Another possibility is to associate the τ_z mode with the Raman band at 64 cm^{-1}, the corresponding band in the d_5 derivative spectrum being at 59.5 cm^{-1} (Figure 2). Thus, Raman bands at 62 and 63 cm^{-1} observed for CpMnT and the CpMnT-d_5 derivative, respectively, should correspond to the T′ mode and the band at 59.5 cm^{-1} for CpMnT can be associated with R′$_z$, its counterpart in the d_5 derivative being at 50 cm^{-1}. The corresponding isotopic ratio values should then be equal to 1.08 and 1.05 for torsion and libration, respectively. These values are larger than those expected for torsional and librational modes (1.078 and 1.03 for τ_z and R$_z$′, respectively), and this suggests that these two modes are coupled and that the Raman bands at 64 and 52.5 cm^{-1} should correspond to an hybrid mode involving libration and torsion. In any case we are led to attribute two strong Raman bands to R$_z$′ and τ_z which should be inactive in the approximation of C_{3v} and C_{5v} local symmetries for M(CO_3) and M$(\eta^5\text{-}C_5H_5)$ groups, respectively. In fact the molecular symmetry is only C_s, and although the intensity of the band associated with the torsion τ_z is expected to be weak insofar as this mode generally involves a small polarizability variation, it can be enhanced in the condensed state because of the distortion of the molecule in the crystal as pointed out by the diffraction study. This increase of the band intensity is observed also in $(\eta^5\text{-}C_5H_5)_2Ni$[2] and Cr$(CO)_3(\eta^6\text{-}C_6H_6)$.[3]

However, one must keep in mind that our interpretation of spectra are based essentially on isotopic substitution effects, and some authors, e.g., Cavagnat et al.,[22] have observed that the torsional motion of the methyl groups does not obey this rule. However, it seems that the isotopic rule is obeyed for all organometallic molecular crystals that we have studied.[2-5] Finally it seems more realistic to place the torsion τ_z at a frequency higher than that of the libration, if one considers that the torsional frequency is determined by the intra- plus intermolecular forces, while the librational frequency is only governed by intermolecular forces identical with those involved in the torsional mode.

b. In the *far-infrared spectrum* of CpMnT at 100 K, three broad bands at 111, 124, and 145 cm^{-1} are observed between 100 and 150 cm^{-1} instead of the ten expected with the C_{2h} factor group with $Z = 4$ (Table I). Consequently it is difficult to propose a definitive assignment. However the comparison with the Raman spectra allows us to attribute the IR band at 145 cm^{-1} to a bending mode δ(R–M–$(CO)_3$) and those at 111 and 124 cm^{-1} to the δ (CMC) mode. The bands at lower frequencies 75, 69, andd 42 cm^{-1}, can tentatively be associated with the Raman bands with similar frequencies. These assignments are summarized in Table II.

The absence of systematic coincidences between Raman and IR frequencies measured at 100 K is in agreement with the crystal structure described by a centrosymmetric space group C_{2h}.

2. Potential Functions Associated with Molecular Reorientational Motions in the Solid State. As we have shown for Cr$(CO)_3(\eta^6\text{-}C_6H_6)$ and Cr$(CO)_3(\eta^5\text{-}C_4H_4S)$ the torsional frequency is determined in the solid state by a potential

(22) Cavagnat, D. Thèse, Doctorat d'Etat, Université de Bordeaux, 1981.

function that can be written as[3,4]

$$V_{\tau_z} = V_{\tau_z}^{\text{intra}} + V_{R_z'}^{\text{inter}}(M(CO)_3) + V_{R_z'}^{\text{inter}}(C_5H_5) \ldots \quad (1)$$

The different terms in this expression will now be analyzed separately.

a. Intramolecular Torsional Potential Function: $V_{\tau_z}^{\text{intra}}$. This term describes the potential energy variation of the "isolated molecule" in the crystal when the C_5H_5 ring executes a rotation around the principal molecular axis. In a first approximation, this function can be represented by the expression

$$2V = V_n^\circ(1 - \cos(n\theta))$$

The potential order n is taken as equal to 15, insofar as the $2\pi/15$ rotation of the C_5H_5 ring or $M(CO)_3$ group keeps $V_{\tau_z}^{\text{intra}}$ invariant. So the minima of the potential function corresponding to different equilibrium positions of the ring $2\pi/15$ distant from each other are equivalent (Figure 4).

Assuming that the torsional motion is harmonic, the potential barrier $V^\circ_{\tau_z}{}^{\text{intra}}$ is given by the relationship

$$V^\circ_{\tau_z}{}^{\text{intra}} = 0.71\frac{\nu_{\tau_z}^2}{n^2}I_r$$

where ν_{τ_z} is the torsional frequency in the isolated state and I_r is the reduced moment of inertia of the molecule.

This potential barrier is expected to be weak in this family of organometallic crystals (e.g., in ferrocene $((\eta^5\text{-}C_5H_5)_2Fe)$ the internal barrier of the molecule in the gas state is 4 kJ mol^{-1}).[23] Moreover in the present case, the high order of the potential function ($n = 15$) decreases to a large extent the value of $V^\circ_{\tau_z}{}^{\text{intra}}$, and we can consider in a first approximation that this term is negligible when compared with other terms in the V_{τ_z} expression (eq 1).

b. Intermolecular Potential Function Associated with Librational Motion. This potential function associated with reorientational motion of the whole molecule around the principal molecular axis is the sum of two terms. The first term takes into account the interaction of the $M(CO)_3$ group with the rest of the atoms in the crystal and the second term considers the interaction of the ring with other atoms. It can be written as

$$V_{R_z'}^{\text{inter}} = V_{R_z'}^{\text{inter}}(M(CO)_3) + V_{R_z'}^{\text{inter}}(C_5H_5) \ldots \quad (2)$$

when one considers in-phase rotation of the aromatic ring with the $M(CO)_3$ group, i.e., when the potential function for the libration of the molecule in the crystal can be written in a first approximation as

$$2V_{R_z'}^{\text{inter}} = V^\circ_{R_z'}{}^{\text{inter}}(1 - \cos(n\theta)) \quad (3)$$

where

$$V^\circ_{R_z'}{}^{\text{inter}} = 0.71\frac{\nu_{R_z'}^2}{n^2}I_z$$

As we have shown for $Cr(CO)_3(\eta^6\text{-}C_6H_6)$,[3] in the $V_{R_z'}^{\text{inter}}$ expression the first term of threefold order is likely the dominant one and must govern the $2\pi/3$ reorientational jumps of the whole molecule in the crystal around its principal axis. However this process leading to three distinguishable molecular configurations is not consistent with the calorimetric results. As already stated the very weak anomaly observed on the C_p curve[1,18] is not interpreted in terms of the existence of distinguishable configurations in the crystal. However this remark remains true whatever the jump angles are. Consequently, one can reasonably exclude any motions of the molecule as a whole; this is confirmed by the high value of the associated potential energy. The potential barrier corresponding to the librational motion can be deduced from the librational frequency according to eq 3. At 5 K, with $\nu_{R_z'} = 52.5$ cm^{-1} and $n = 3$ one finds $V^\circ_{R_z'}{}^{\text{inter}} \simeq 100$ kJ mol^{-1}. For $Cr(CO)_3(\eta^6\text{-}C_6H_6)$, this barrier is equal to 67 kJ mol^{-1}.

As a conclusion the remaining possible reorientational motions are those involving the C_5H_5 rings alone.

c. Potential Function Associated with the Reorientational Motion of One Aromatic Ring in the Crystal. In the crystal, the equilibrium positions of the ring corresponding to the minima, V_1, V_2, and V_3 (Figure 4) of the potential function are distinguishable, while V_1 and V_4, separated by $2\pi/5$, are equivalent. Thus, in agreement with calorimetric results, we can exclude the $2\pi/15$ jumps of the ring, only the $2\pi/5$ ring reorientations taking place; consequently the corresponding potential function is of fivefold order.

In eq 1, giving V_{τ_z}, it is not possible to estimate separately the different terms. However several reasonable assumptions can be made:

(1) The torsional mode is attributed to the Raman band at 64 cm^{-1}. It implies that the $M(CO)_3$ group remains fixed during this motion in order to explain the high value of the isotopic frequency ratio ($\rho \sim 1.08$). This agrees with the conclusions obtained for $Cr(CO)_3(\eta^6\text{-}C_6H_6)$.[3] Thus the moment of inertia, which has to be considered in the expression of $V^\circ_{\tau_z}$ is that of the C_5H_5 ring instead of the reduced moment I_r of the two moieties of the molecule. In this condition, the potential function governing the reorientation of the C_5H_5 ring is given by

$$V_{reo}(C_5H_5) = V_{\tau_z}^{\text{intra}} + V_{R_z'}^{\text{inter}}(C_5H_5)$$

with

$$2V_{R_z'}^{\text{inter}}(C_5H_5) = V^\circ_{R_z'}{}^{\text{inter}}(1 - \cos(n\theta))$$

and

$$V^\circ_{R_z'}{}^{\text{inter}}(C_5H_5) = 0.71\frac{\nu_{\tau_z}^2}{n^2}I_z(\text{ring})$$

(2) The term $V_{\tau_z}^{\text{intra}}$ is, as already stated in section IV.2.a, most likely neglibible; moreover, even if it was considered as only responsible for the torsional frequency in the solid state, one should derive a $V^\circ_{\tau_z}{}^{\text{intra}} = 0.71(64^2/15^2)I_z(\text{ring}) = 1.5$ kJ mol^{-1}. Thus, this term, which is overestimated in this calculation, is nevertheless much smaller than $V^\circ_{R_z'}{}^{\text{inter}}(C_5H_5)$, which can be deduced from the same frequency but uses $n = 5$ for the intermolecular forces.

$$V^\circ_{R_z'}{}^{\text{inter}}(C_5H_5) = 0.71\frac{64^2}{5^2}I_z(\text{ring}) = 12.5 \text{ kJ mol}^{-1}$$

At 300 K the torsional frequency is strongly lowered, and this barrier becomes equal to about 10 kJ mol^{-1}.

Recently, Berar et al.[17] have performed calculations of the lattice energy for $Mn(CO)_3(\eta^5\text{-}C_5H_5)$. They have proposed an intermolecular potential barrier for one C_5H_5 ring reorientation equal to 5 kJ mol^{-1}. This value, although two times lower than that obtained in our study, is of a similar order of magnitude. Figure 5 shows a schematic representation of V_{reor} corresponding to the following situations. (i) $V_{\tau_z}^{\text{intra}}$ and $V_{R_z'}^{\text{inter}}$ are in phase. This corresponds to molecular conformation C_s in the solid ($\alpha_1 = \alpha_2 = 12°$, Figure 4); $V^{\circ\text{intra}}$ is arbitrarily overestimated and is equal to 2 kJ mol^{-1}. (ii) The minima of $V_{\tau_z}^{\text{intra}}$ and $V_{R_z'}^{\text{inter}}$ are displaced by about 5°. This situation corresponds to a C_1 site symmetry of the molecule in the unit cell according to crystallographic studies.[11,20] The resulting potential curve exhibits a small asymmetry, which can be associated with the weak anomaly observed on the C_p curve (see section V). In any case, the potential barrier $V^\circ_{reor}(C_5H_5)$ obtained from Figure 5 is about 14 kJ mol^{-1} and is not very different from the activation energy deduced from quasi-elastic

(23) Haaland, A.; Nelson, J. E. *Acta Chem. Scand.* **1968**, *22*, 2653.

neutron scattering experiments;[7] this convergence favors our model.

V. Dynamics of C_5H_5 Rings

Figures 2 and 3 show that the temperature dependence of the Raman spectra of CpMnT and CpReT is very similar. Moreover, from crystallographic studies, the two compounds have the same crystal structure at 300 K and at 77 K.[17,24] Thus we think that for both compounds the dynamic disorder investigated by vibrational spectroscopy involves the same mechanism. Because of the lack of data on CpReT obtained by other techniques such as NMR or IQNS, this discussion is mainly devoted to $Mn(CO)_3(\eta^5C_5H_5)$.

The studies of the dynamics of the C_5H_5 rings are based on the one hand, on the temperature dependence of the low-frequency Raman modes, in particular those associated with the torsional and librational modes, and on the other hand, on the results that we have obtained for $Mn(CO)_3(\eta^5\text{-}C_5H_5)$ by quasi-elastic neutron scattering experiments. The broadening of the quasi-elastic peak observed at about 300 K has been interpreted in terms of dynamic disorder and has been fitted by using $2\pi/5$ rotational jumps of C_5H_5 rings around the principal molecular axis.[7]

As for $(\eta^5C_5H_5)_2Ni$, the lower part of the potential function curve for the C_5H_5 ring reorientation (Figure 5) can be approximated by a parabola of an harmonic oscillator, which can be used to describe the oscillations of C_5H_5 rings at low temperature.

As soon as the vibrational quantum number approaches $v = 4$, the torsional motion becomes a motion of large amplitude. One can consider that, at a given temperature, e.g., 100 K, an important proportion of the rings execute large amplitude oscillations around an average equilibrium position slightly displaced from the equilibrium position of the rings in a low vibrational state oscillating with a small amplitude. This situation can be seen in Figure 5d. The weak anomaly observed on the C_p curve by calorimetry in the temperature range 75–130 K could be interpreted as the transition from a small to a large amplitude oscillatory state of the aromatic ring centered around slightly displaced equilibrium positions.

1. Temperature Effect on Spectra. Figure 6 shows the frequency variations of some Raman bands as a function of temperature. All frequencies decrease when the temperature is raised. The torsional and bending low-frequency modes are the most sensitive ones, especially in the temperature range above 100 K, where a weak anomaly on the C_p curve is observed by calorimetry.

Figure 7 represents the temperature dependence of the Raman band half-widths of external and internal bending modes between 5 and 250 K. All Raman bands broaden when the temperature is raised. This is particularly true for the torsion τ_z and the external modes. The broadening reaches about 6 cm^{-1} at 170 K for torsional and translational modes.

The different causes of band broadening have already been listed in our previous publication on metallocenes.[2] Among these causes, the reorientational process of the C_5H_5 rings can account for the broadening of the torsional mode τ_z, the activation energy of the process being given by the relation

$$\Delta\nu_{1/2} = (a + bT) + C\nu_0 e^{-Ea/kT}$$

The first term represents the anharmonicity effect, which can be estimated from the low-temperature linear part of the experimental curve: $\Delta\nu_{1/2} = f(T)$ (Figure 7). The second term represents the thermally activated phenomenon, characterized by an activation energy E_a and the frequency (preexponential factor) ν_0. The activation energy obtained by fitting the experimental curve $\Delta\nu_{1/2} = f(T)$ for the torsion τ_z with the above relation after substracting the anharmonicity effect is about 1.7 kJ mol^{-1}. The comparison of this value with $V^\circ_{reor}(C_5H_5)$ ($\sim$14 kJ mol^{-1}) shows that this activation energy is too low to be identified with the potential barrier that the C_5H_5 ring must overcome to undergo the $2\pi/5$ reorientation.

When one introduces the value of V°_{reor} (14 kJ mol^{-1}) in the Arrhenius relation, one expects a broadening of 0.2 cm^{-1} for the torsional mode at 300 K. This value is too small when compared to experimental broadening. Therefore the thermally activated jumps cannot be invoked to explain the broadening of the Raman band. Anharmonic terms of higher order could be responsible for these broadenings. We have fitted the experimental curve $\Delta\nu_{1/2} = f(T)$ for τ_z by the expression $aT + bT^2$ in which aT and bT^2 represent the contributions of the cubic and quartic anharmonic terms, respectively.[25] The best fit can be obtained for a set of parameters, $a = 0.16 \times 10^{-1}$ and $b = 0.76 \times 10^{-4}$.

A large broadening is also observed for the translational modes and internal bending modes δ(CMC) and δ(R–M–$(CO)_3$) (Figure 7). For the translational mode T′, which is generally a dispersive mode, the broadening can reflect the projected density of state in the case of the presence of a static disorder in the crystal. However, the proportion of molecules in the state of jumps that can be calculated by the Boltzman relation is about $N/N_0 = e^{-V^\circ/kT} = 0.02$ at 300 K. This value indicates that the rate of disorder induced by ring jumps is small and cannot be retained among the causes of broadening associated with the breakdown of $k = 0$ selection rules. Thus, one must consider that anharmonicity is the main cause of the broadening of bands associated with external modes, especially when the melting point is approached. The vibrational dephasing can also account for a part of the causes of broadening for some internal modes in particular.

In conclusion, the activation energy deduced from the curve $\Delta\nu_{1/2} = f(T)$ and associated with the torsion does not correspond to a ring jump process but is connected with large amplitude motions of C_5H_5 rings. This can explain the small anomaly on the C_p curve observed by calorimetry. Moreover, we must emphasize that the large amplitude motion and therefore the anharmonicity appears as a consequence of the low potential barrier. In others words, the broadening of a Raman band, which is due to anharmonic terms, expresses the existence of a low potential barrier and thus the possibility of the C_5H_5 jumps.

Finally, the potential barrier V°_{reor} that one C_5H_5 ring must overcome to execute $2\pi/5$ jumps is 10 kJ mol^{-1}, obtained from the torsional frequency. This is slightly lower than that deduced from quasi-elastic neutron scattering experiments (E_a= 16.7 kJ mol^{-1}). Consequently the difference between the correlation times obtained by these two techniques must not be significant. If we introduce the potential barrier V°_{reor} of ring reorientation in the expression $\tau_c^{-1} = C\nu_0 e^{-V^\circ_{reor}/kT}$, one finds $\tau_c = 2.7 \times 10^{-11}$ s at 300 K, when the preexponential factor is taken as equal to the torsional frequency ($\sim$55 cm^{-1}). This value of τ_c compares quite well with neutron scattering results, which give $\tau_c = 1.7 \times 10^{-11}$ s. However, this value of τ_c is much larger than the correlation time deduced from the spin–lattice relaxation time T_1($\tau_c = 6.4 \times 10^{-13}$ s) by Fitzpatrick et al.[9] and associated with an activation energy equal to 7.2 kJ mol^{-1}.

Registry No. CpMnT, 12079-65-1; CpMnT-d_5, 88295-81-2; CpReT, 12079-73-1.

(24) Chhor, K.; Calvarin, G., unpublished results.

(25) Sood, A. K.; Aroba, A. K.; Umadevi, V.; Venkataraman, G. *Pramana* **1981**, *16*, 1.